Theoretical Determination of a Thermogravimetric Model of Oak Cork (*Quercus variabilis*) Using Málek Kinetic Analysis

Weiwei Shangguan
Zhangjing Chen
Xiaozhou Song
Yafang Lei

Abstract

The purpose of this study was to determine the expression of a kinetic model and the determination of kinetic parameters for cork. Thermal analysis kinetics of cork and impurities (sclereids and lenticels) were studied by thermogravimetric (TG) curves. The Málek method was used to obtain kinetic parameters in this experiment. Reconstruction models of $y(\alpha)$ and $z(\alpha)$ were compared with standard curves to determine appropriate kinetic models. The results showed that the RO(n) model was suitable to describe the dynamic process of cork, sclereids, and lenticels. The expressions of kinetic models were $f(\alpha) = (1 - \alpha)^{4.89}$ for cork, $f(\alpha) = (1 - \alpha)^{5.82}$ for sclereids, and $f(\alpha) = (1 - \alpha)^{5.00}$ for lenticels. The natural log values ln A were 19.56, 28.90, and 28.88 ln s^{-1} for cork, sclereids, and lenticels, respectively. Fitting errors of parameters for cork, sclereids, and lenticels were less than 5 percent. The fitted conversion rate and curves of mass fraction were in good agreement with experimental data. Obtaining the kinetic model and parameters provides a basis for prediction of thermal properties of cork.

Cork is a natural material obtained from the phellem layer of cork oak. There are mainly two categories of cork oak. *Quercus suber* is located in the Mediterranean region, and *Quercus variabilis* is in China. The bark of cork oak can be stripped every 15 to 20 years without affecting tree health (Luo et al. 2009). Cork production in Europe accounts for 80 percent of world production, especially for Portugal (Silva et al. 2005). Over the last 1,000 years, cork has had the reputation of having a low density, high elasticity, good thermal insulation, good acoustic insulation, flame retardancy, and abrasion resistance. Cork can be used as an insulating layer and heat shield in and during cold storage as advanced building components (Luo et al. 2009), and space in vehicles (Pereira 2007) because of its high heat insulation performance.

Cork that is first produced from the first periderm is called virgin cork. Sclereids and lenticels occur more frequently in virgin cork than in second cork (Zhao 2012), which is from the newly produced phellem layer. Sclereids are lignified sclerenchyma cells, also known as a stone cell. Intercellular open spaces exist in lenticels that exchange gas with air (Pereira 2007). Sclereids and lenticels have great impact on processing and utilization of cork. Sclereids accelerate tool wear owing to hard material texture and high density. Lenticels make the sliced cork tear considerably, causing significant surface scratches (Zhao et al. 2013). At present, there have been many studies on cork; however, reports on the effect of sclereids and lenticels on cork quality are rare.

With the development of science and technology, especially the rise of space technology, effective methods for evaluating the thermal stability and service life for polymer materials are needed. Thermal analysis was first used to study reaction kinetics in the 1920s and was

The authors are, respectively, Lecturer, College of Forestry, Northwest A&F Univ., Shaanxi, China (shangguan_weiwei@163.com); Research Professor, Dept. of Wood Sci. Forest Products, Virginia Polytechnic Inst. State Univ., Blacksburg (chengo@vt.edu); and Professor and Professor, College of Forestry, Northwest A&F Univ., Shaanxi, China (songxiaozhou@nwsuaf.edu.cn [corresponding author], leiyafang@sina.com). X. Song and Y. Lei contributed equally to this work. This paper was received for publication in February 2017. Article no. 17-00012.

Forest Prod. J. 67(7/8):481–486.
doi:10.13073/FPJ-D-17-00012

developed in the 1950s (Vyazovkin and Wight 1998, Hu et al. 2008). This method is used to study the reaction kinetics of solid matter under linear heating conditions. With a single thermal analysis curve, it is difficult to determine the reaction mechanism. The activation energy and order of reaction are calculated from a single experimental curve using the Freeman and Carroll (1958) method. However, the linear relationship between E and ln A (E is activation energy and A is preexponential factor) makes them covary. Therefore, all kinetic parameters obtained from a single experimental curve are somewhat problematic (Šesták and Málek 1993). The Málek method solves the above problem by obtaining these parameters separately. It calculates the activation energy by an iso-conversional method and then reconstructs the kinetic curve. The kinetic model can be determined from these reconstruction curves, and a preexponential factor related to the selected models can be obtained (Málek 1989, 1992, 1993; Málek and Smrčka 1991; Málek et al. 2001). The Málek method has been applied in glassy germanium disulfide (Málek 1989), chalcogenide glasses (Málek 1989), zirconium dioxide (Málek et al. 2001), and natural fibers (Yao et al. 2009). Activation energy and preexponential factors have been obtained from one single thermal analysis curve for cork (Wei and Xiang 2010). However, kinetic parameters of cork, sclereids, and lenticels using Málek's method have not been reported.

The thermodynamic analyses of cork, sclereids, and lenticels at different heating rates were studied to obtain the basic information that may differ from wood. The Málek method was used in this experiment to develop reconstruction models of $y(\alpha)$ and $z(\alpha)$, which were further used to determine kinetic models of $f(\alpha)$ for cork and impurities. The objective of this study was to determine the kinetic model of $f(\alpha)$ and kinetic parameters of A and n. This work can help understand pyrolysis characteristics of cork, sclereids, and lenticels, providing the theoretical foundation for processing and utilization of cork.

Kinetic Methods

The dynamic equation for a solid state reaction has been described by Málek (1992) and Hu et al. (2008)

$$\frac{d\alpha}{dt} = A\exp(-x)f(\alpha) \tag{1}$$

where α is conversion rate, t is time (s), A is preexponential factor (s^{-1}), x is reduced activation energy, and $f(\alpha)$ is kinetic model.

The conversion rate of α is calculated as

$$\alpha = \frac{w_0 - w_t}{w_0 - w_f} \tag{2}$$

where w_0 is sample weight at initial time, w_t is weight at time t, and w_f is final weight.

$$x = \frac{E}{RT} \tag{3}$$

where E is activation energy (kJ/mol), R is universal gas constant (8.314×10^{-3} kJ/mol), and T is absolute temperature (K).

Under nonisothermal conditions, the temperature rises at a constant heating rate β (°C/min). Integrating Equation 1, we obtain

$$\int_0^{\alpha} \frac{d\alpha}{f(\alpha)} = g(\alpha) = \frac{AE}{\beta R} e^{-x}\left[\frac{\pi(x)}{x}\right] \tag{4}$$

where $\pi(x)$ is an approximation of the temperature integral. According to previous studies, the rational expression of Senum-Yang is appropriate as follows (Senum and Yang 1977, Málek 1992):

$$\pi(x) = \frac{x^3 + 18x^2 + 88x + 96}{x^4 + 20x^3 + 120x^2 + 240x + 120} \tag{5}$$

Kinetic models of $f(\alpha)$ and $g(\alpha)$ can be determined by defined functions of $y(\alpha)$ and $z(\alpha)$ using the Málek method. The functions of $y(\alpha)$ and $z(\alpha)$ are as follows (Yao et al. 2009):

$$y(\alpha) = \frac{d\alpha}{dt} e^{x} = Af(\alpha) \tag{6}$$

$$z(\alpha) = \pi(x)\frac{d\alpha}{dt}\frac{T}{\beta} = f(\alpha)g(\alpha) \tag{7}$$

Experimental data of thermal analysis were collected and were substituted into Equations 6 and 7. After normalization within the interval between 0 and 1, the shapes of $y(\alpha)$ and $z(\alpha)$ were obtained. The mechanism functions of $f(\alpha)$ and $g(\alpha)$ were then determined after comparing experimental curves of $y(\alpha)$ and $z(\alpha)$ with the standard curves (Málek 1992).

Materials and Methods

Bark of *Q. variabilis*, virgin cork, was collected from mature trees (50 yr old) and harvested in China. Cork, sclereids, and lenticels were separated manually from the bark. Cork, sclereids, and lenticels were ground and screened with a 40- to 60-mesh sieve. The moisture content of cork was 6 percent.

A thermogravimetric analyzer (TA-60WS made by Shimadzu Company in Japan) was used to analyze the cork materials. The powder was distributed in the sample pan, and the initial weight of the cork was 4 mg owing to low density; sclereids and lenticels were 9 to 10 mg. Measurements of the thermokinetics were in an atmosphere of nitrogen of 50 mL/min. Thermogravimetry (TG) curves were obtained in the range of 25°C to 1,000°C at heating rates of 10°C/min, 20°C/min, and 30°C/min. Data processing and parameter calculation were determined using MATLAB software.

Results and Discussion

Determination of the $f(\alpha)$ function

Thermal kinetic models of $f(\alpha)$ corresponding to various mechanisms are summarized in Table 1. The Johnson-Mehl-Avrami (n) (JMA[n]) model is based on the assumption of nucleation and growth processes. The simplified geometry of the diffusion process is expressed by two-dimensional diffusion (D2), Jander equation (D3), and Ginstling-Brounshtein (D4) models. Reaction order (n) (RO[n]) and Šesták-Berggren (m,n) (SB[m,n]) models are empirical kinetic models (Málek et al. 2001). It is possible to determine the appropriate model for the materials because there is a large difference of parameters among different kinetic models (Málek and Criado 1994).

Table 1.—Summary of thermal kinetic models.

Model	Symbol	$f(\alpha)$	$g(\alpha)$
Johnson-Mehl-Avrami	JMA(n)	$n(1-\alpha)[-\ln(1-\alpha)]^{1-1/n}$	$[-\ln(1-\alpha)]^{1/n}$
2D-diffusion	D2	$1/[-\ln(1-\alpha)]$	$\alpha + (1-\alpha)\ln(1-\alpha)$
Jander equation	D3	$(3/2)(1-\alpha)^{2/3}[1-(1-\alpha)^{1/3}]^{-1}$	$[1-(1-\alpha)^{1/3}]^2$
Ginstling-Brounshtein	D4	$(3/2)[(1-\alpha)^{-1/3}-1]^{-1}$	$1-(2/3)\alpha-(1-\alpha)^{2/3}$
Reaction order	RO(n)	$(1-\alpha)^n$	$[1-(1-\alpha)^{1-n}]/(1-n)$
Šesták-Berggren	SB(m,n)	$\alpha^m(1-\alpha)^n$	

The $f(\alpha)$ function can be determined from a nonisothermal curve if activation energy is known (Málek 1989). In order to accurately determine the activation energy, both the Friedman and Flynn-Wall-Ozawa (FWO) methods were applied to calculate the activation energy of cork and its impurities. Activation energy values using the Friedman method and FWO method were calculated according to Tian et al. (2016). They were calculated as α values between 0.2 and 0.6 because they were stable in this range according to our previous study (Shangguan et al. 2018). The average activation energies of three heating rates using Friedman and FWO methods are shown in Table 2. The activation energies of cork and impurities were lower than those of natural fibers, with an average value of 161.8 kJ/mol (Yao et al. 2008). It is probably because of suberin in cork and impurities (Zhao 2012). The activation energies of impurities were closer to natural fibers, and they are mainly composed of holocellulose and lignin (Yao et al. 2008, Zhao 2012).

The experimental data of cork and impurities at different heating rates were substituted into Equations 6 and 7. The shapes of $y(\alpha)$ and $z(\alpha)$ after normalization were then determined. According to Equations 6 and 7, the shape of the function $f(\alpha)$ is related to $y(\alpha)$ and $z(\alpha)$. The shapes of $y(\alpha)$ and $z(\alpha)$ functions are quite different, and they are sensitive to subtle changes in the kinetic model of $f(\alpha)$ (Málek et al. 2001). At the same time, $y(\alpha)$ and $z(\alpha)$ functions are not affected by the heating rate. Thus it is reliable to use reconstruction models of $y(\alpha)$ and $z(\alpha)$ to guide the choice of a suitable kinetic model of $f(\alpha)$ (Málek 1989).

The functions $y(\alpha)$ and $z(\alpha)$ for cork, sclereids, and lenticels have similar curves. In Figure 1, $y(\alpha)$ and $z(\alpha)$ curves of cork at different heating rates overlapped. Figure 1 also shows that $y(\alpha)$ and $z(\alpha)$ functions are independent of heating rate (Málek and Smrčka 1991). Curves of $y(\alpha)$ were concave shapes, and the maximum values were at $\alpha_M = 0$. The function $z(\alpha)$ presented convex curves, and the maximum values were at $\alpha_p{}^\infty$, which were shown in Table 3. The parameter α_p is the conversion rate at the maximum of the differential thermal gravity (DTG) peak. A combination of Figure 1 and Table 3 allows for the determination of the most suitable kinetic model for cork and its impurities. The thermal kinetic model of $f(\alpha)$ was limited to D2, D3, D4, RO($n > 1$), and JMA($n < 1$) models because $\alpha_M = 0$ and convex shapes of $y(\alpha)$ (Málek 1992). The $\alpha_p{}^\infty$ values of cork and impurities in Table 3 were less than 0.628. This determined that the RO($n > 1$) model was the most suitable model for thermal degradation kinetics of cork and impurities (Málek 1992, Hu and Shi 2001). The RO model is used to describe the process in which the $y(\alpha)$ curve decreases with conversion rate (Málek 1989). This is the same as the natural fibers, which showed RO($n > 1$) is the appropriate model for fibers (Yao et al. 2009).

Table 2.—Average activation energies of cork and impurities at α between 0.2 and 0.6.[a]

	Activation energy (kJ/mol)		Average activation energy (kJ/mol)
	Friedman method	FWO method	
Cork	116.10 (12.40)	97.01 (5.54)	106.55
Sclereids	147.44 (7.05)	138.94 (10.00)	143.19
Lenticels	157.01 (13.89)	131.30 (10.75)	144.15

[a] Values in parentheses denote standard deviation from three heating rates. FWO = Flynn-Wall-Ozawa.

Determination and evaluation of kinetic parameters

The activation energy and kinetic parameters of cork were calculated from one experimental TG curve (Wei and Xiang 2010). However, the kinetic parameter of the preexponential factor and activation energy influence each other from the expression of $\ln A = a + bE$ (a and b are constants; Šesták and Málek 1993). This problem can be solved by calculating the activation energy in advance. Kinetic parameters obtained by the Málek method are based on selected models and known activation energy (Málek 1989, Málek and Smrčka 1991, Málek et al. 2001).

After obtaining the expression of kinetic models of $f(\alpha) = (1-\alpha)^n$ and $g(\alpha) = [1-(1-\alpha)^{1-n}]/(1-n)$, an equation of α during thermogravimetric analysis can be obtained by combining $g(\alpha)$ and Equation 4:

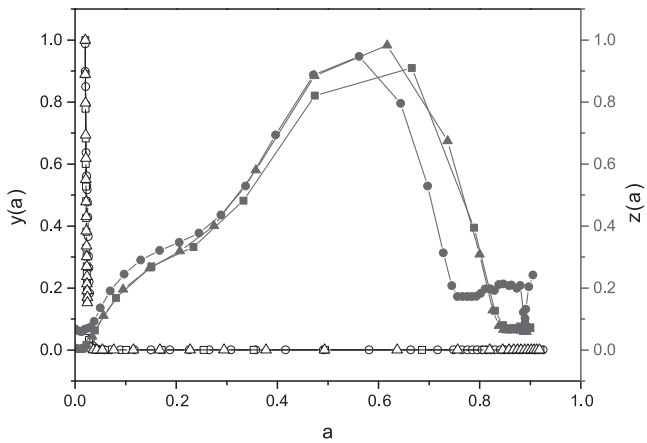

Figure 1.—Relation curves of y(α)-α and z(α)-α for cork at different heating rates. Symbols of ○, □, and △ represent heating rates of 10°C/min, 20°C/min, and 30°C/min for y(α)-α curves. Symbols of ●, ■, and ▲ represent heating rates of 10°C/min, 20°C/min, and 30°C/min for z(α)-α curves.

Table 3.—Values of α_M, α_p, and $\alpha_p\infty$ for cork and impurities.[a]

	α_M	α_p	$\alpha_p\infty$
Cork	0	0.555 (0.021)	0.573 (0.024)
Sclereids	0	0.610 (0.017)	0.628 (0.009)
Lenticels	0	0.583 (0.038)	0.602 (0.027)

[a] Values in parentheses denote standard deviation from three heating rates.

$$\alpha(T) = 1 - \left[1 - T\frac{\pi(x)}{\beta}(1-n)Ae^{-x}\right]^{1/(1-n)} \quad (8)$$

The parameters A and n can be obtained after fitting experimental data into Equation 8 for the known activation energies.

From Table 4, the expressions of the kinetic models were $f(\alpha) = (1-\alpha)^{4.89}$ for cork, $f(\alpha) = (1-\alpha)^{5.82}$ for sclereids, and $f(\alpha) = (1-\alpha)^{5.00}$ for lenticels. Compared with the thermal analysis of a single curve, the value of ln A for cork using the Málek method was slightly higher than 18.46 s^{-1} for Yunnan cork and 18.30 s^{-1} for Hubei cork (Wei and Xiang 2010). The natural log values (ln A) of cork and impurities were generally less than natural fibers, with an average value of 38.24 s^{-1} (Yao et al. 2009). Values of n for cork and impurities were higher than for natural fibers except rice straw at 5.81 (Yao et al. 2009). As can be seen from the above data, a difference in kinetic parameters existed between cork and lignocellulose materials. This difference is probably due to differences in chemical composition. The content of suberin is higher in cork than in sclereids and lenticels but not in lignocellulose materials (Zhao 2012). The degree of fit between the experimental and calculated data was obtained by the least square method (Yao et al. 2009) in Table 4. The error did not exceed 5 percent, which met the demand of the kinetic exponent (Málek and Criado 1994). Fitted curves of $\alpha - t$ at different heating rates were obtained after the parameters (Table 4) were substituted into Equation 8. The experimental data and fitted curves of α for cork are shown in Figure 2 with good agreement. Good fitting curves of sclereids and lenticels are not shown here.

Although the fitting errors were controlled within 5 percent, it is still not sufficient to evaluate the kinetic models by the least square method. This is because different functions of $f(\alpha)$ can be fitted using E and A (Vyazovkin 1992, Koga 1994). Another method was used to evaluate kinetic models and parameters in this situation (Pérez-Maqueda et al. 2006, Yao et al. 2009). The following equation can be obtained after transforming Equation 1:

$$\ln\left[\frac{d\alpha/dt}{f(\alpha)}\right] = \ln cA - \frac{E_a}{RT} \quad (9)$$

By substituting experimental data ($d\alpha/dt$) and the obtained model of $f(\alpha)$, a single straight line with slope of

Table 4.—Fitting parameters of n *and ln* A *for cork and impurities.*[a]

	n	ln A (s^{-1})	Fit (%)
Cork	4.89 (0.60)	19.56 (0.02)	4.68 (2.39)
Sclereids	5.82 (0.30)	28.90 (0.14)	2.60 (0.29)
Lenticels	5.00 (0.29)	28.88 (0.13)	2.51 (0.42)

[a] Values in parentheses denote standard deviation from three heating rates.

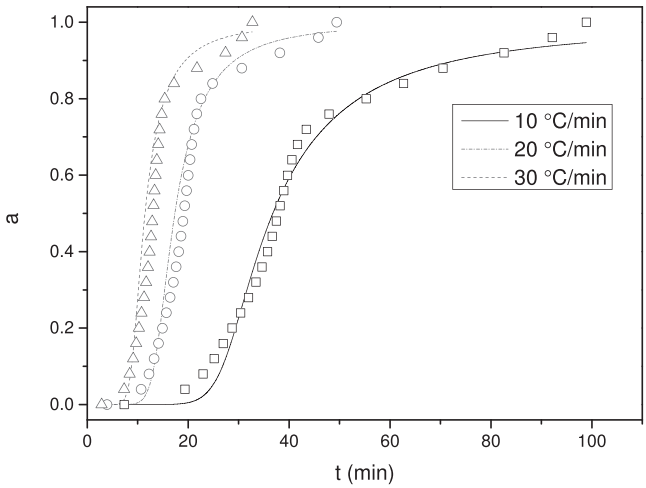

Figure 2.—Comparison of fitted cork curves and experimental data for α.

($-E_a/R$) and intercept of (ln cA) can be obtained while being independent of heating rate. In this study, linear relationships between ln[($d\alpha/dt$)/$f(\alpha)$] and $1/T$ are shown in Figure 3. Straight lines of both cork and impurities overlapped even at different heating rates. Straight lines can also be obtained using inappropriate models in parallel at different heating rates (Pérez-Maqueda et al. 2006). The activation energies of cork, sclereids, and lenticels can be calculated by the slopes of the fitted lines. Activation energies calculated from these slopes were close to those in Table 2. The error of activation energy between the known value (Table 2) and calculated value (Fig. 3) was slightly higher for lenticels; however, the errors of cork and sclereids were around 5 percent.

Predicted curves of mass fraction for cork and impurities

Predicted curves of mass fraction can be obtained from the following equation (Yao et al. 2009):

$$\text{Mass fraction } (\%) = 100\%\left[1 - \alpha_p(T)(1 - \text{residue})\right] \quad (10)$$

where α_p is the calculated conversion rate from Equation 8.

Through determination of parameters, the predicted curves of mass fraction can be obtained after substituting $\alpha_p(T)$ into Equation 10. From Figure 4, the predicted curves of cork fitted well with experimental data (10°C/min), proving the validity of the kinetic parameters calculated with the selected model. The curves of sclereids and lenticels had good fits with experimental data, which are not shown. Selection of thermodynamic model and calculation of model parameters are helpful to the analysis of thermal properties of cork and impurities.

Conclusions

The Málek method was used to obtain thermal kinetic models and kinetic parameters. For cork and impurities, reconstruction curves of $y(\alpha)$ and $z(\alpha)$ showed concave and convex shapes, respectively. The RO($n > 1$) model is an appropriate model for thermokinetic analysis of cork, sclereids, and lenticels. Kinetic parameters of n were 4.89, 5.82, and 5.00 for cork, sclereids, and lenticels, respectively.

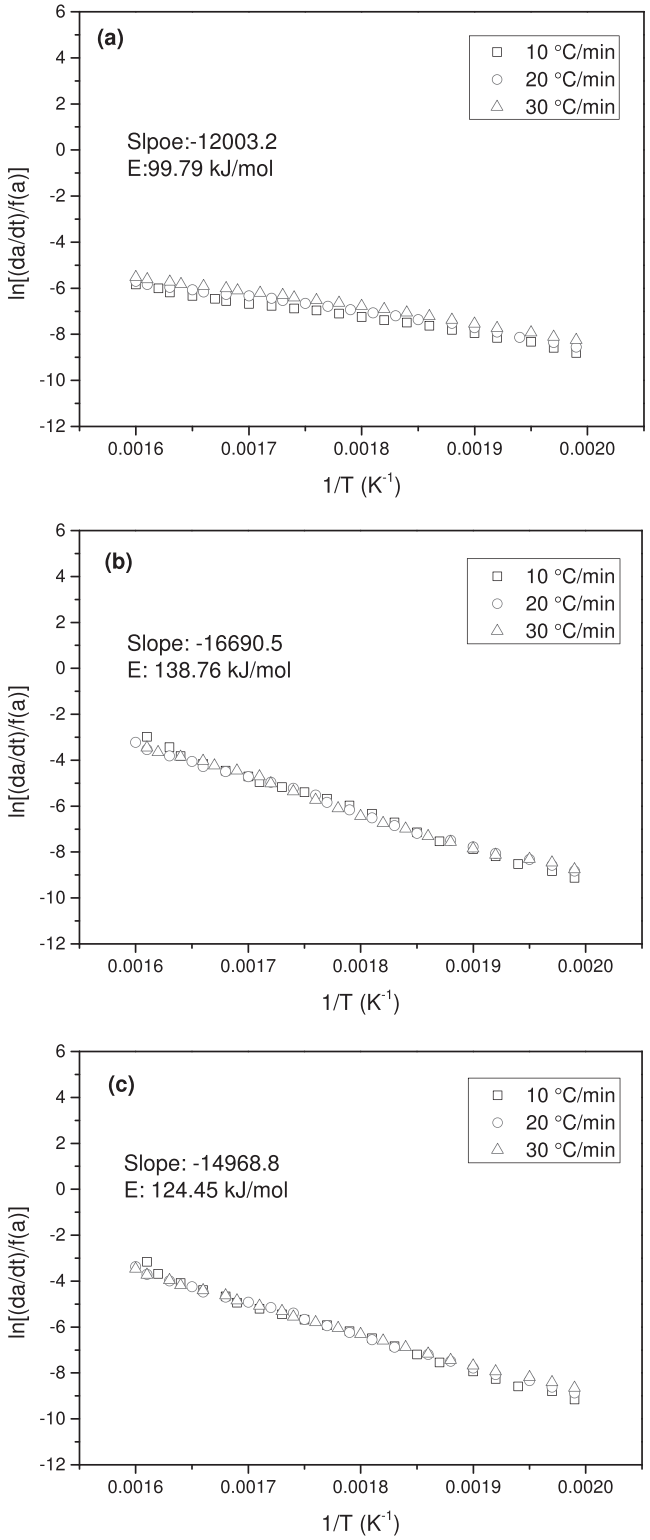

*Figure 3.—Linear relationship between ln[(*dα*/*dt*)/*f(α)] and 1/*T*: (a) cork; (b) sclereids; (c) lenticels.*

The logarithms of the preexponential factor were 19.56, 28.90, and 28.88 s^{-1} for cork, sclereids, and lenticels, respectively. The error was limited to an acceptable range of 5 percent. The curves of linear relationships between ln[(*dα*/*dt*)/*f*(α)] and 1/*T* overlapped at different heating rates for

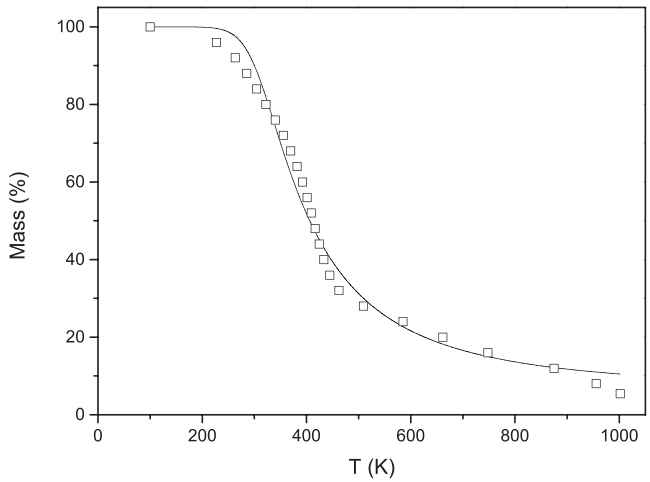

Figure 4.—Predicted curve of mass fraction and experimental data for cork at a heating rate of 10°C/min.

cork, sclereids, and lenticels. Obtained kinetic models and parameters can be used to simulate thermal degradation properties of cork.

Acknowledgments

This research was financially supported by the National Natural Science Foundation of China, Grant No. 31470583. The authors also acknowledge the Fundamental Research Funds for the Central Universities, Grant No. 2452017097.

Literature Cited

Freeman, E. S. and B. Carroll. 1958. The application of thermoanalytical techniques to reaction kinetics. the thermogravimetric evaluation of the kinetics of the decomposition of calcium oxalate monohydrate. *J. Phys. Chem*. 62(4):394–397.

Hu, R. and Q. Shi. 2001. Thermal Analysis Kinetics. Science Press, Beijing.

Hu, R. Z., S. L. Gao, F. Q. Zhao, Q. Z. Shi, T. L. Zhang, and J. J. Zhang. 2008. Thermal Analysis Kinetics. 2nd ed. Science Press, Beijing.

Koga, N. 1994. A review of the mutual dependence of Arrhenius parameters evaluated by the thermoanalytical study of solid-state reactions: The kinetic compensation effect. *Thermochim. Acta* 244(94):1–20.

Luo, W., W. Zhang, and Y. Huang. 2009. *Quercus variabilis* in China. China Forestry Publishing, Beijing.

Málek, J. 1989. A computer program for kinetic analysis of non-isothermal thermoanalytical data. *Thermochim. Acta* 138(2):337–346.

Málek. J. 1992. The kinetic analysis of non-isothermal data. *Thermochim. Acta* 200(92):257–269.

Málek, J. 1993. The thermal stability of chalcogenide glasses. *J. Therm. Anal*. 40(1):159–170.

Málek, J. and J. M. Criado. 1994. A simple method of kinetic model discrimination. Part 1. Analysis of differential non-isothermal data. *Thermochim. Acta* 236(12):187–197.

Málek. J., T. Mitsuhashi, and J. M. Criado. 2001. Kinetic analysis of solid-state processes. *J. Mater. Res*. 16(6):1862–1871.

Málek, J. and V. Smrčka. 1991. The kinetic analysis of the crystallization processes in glasses. *Thermochim. Acta* 186(1):153–169.

Pereira, H. 2007. Cork: Biology, Production and Uses. Elsevier Science, Amsterdam.

Pérez-Maqueda, L. A., J. M. Criado, and P. E. Sanchez-Jimenez. 2006. Combined kinetic analysis of solid-state reactions: A powerful tool for the simultaneous determination of kinetic parameters and the kinetic model without previous assumptions on the reaction mechanism. *J. Phys. Chem. A* 110(45):12456–12462.

Senum, G. I. and R. T. Yang. 1977. Rational approximations of the integral of the Arrhenius function. *J. Therm. Anal*. 11(3):445–447.

Šesták, J. and J. Málek. 1993. Diagnostic limits of phenomenological models of heterogeneous reactions and thermal analysis kinetics. *Solid State Ionics* 63–65(9):245–254.

Shangguan, W., Z. Chen, J. Zhao, and X. Song. 2018. Thermogravimetric analysis of cork and cork components from *Quercus variabilis*. *Wood Sci. Technol*. 52(1):181–192.

Silva, S. P., M. A. Sabino, E. M. Fernandes, V. M. Correlo, L. F. Boesel, and R. L. Reis. 2005. Cork: Properties, capabilities and applications. *Int. Mater. Rev*. 50(6):345–365.

Tian, L., B. Shen, H. Xu, F. Li, Y. Wang, and S. Singh. 2016. Thermal behavior of waste tea pyrolysis by TG-FTIR analysis. *Energy* 103(10):533–542.

Vyazovkin, S. 1992. Alternative description of process kinetics. *Thermochim*. *Acta* 211(92):181–187.

Vyazovkin. S. and C. A. Wight. 1998. Isothermal and non-isothermal kinetics of thermally stimulated reactions of solids. *Int. Rev. Phys. Chem*. 17(3):407–433.

Wei, X. and S. Xiang. 2010. Study on pyrogenation characteristics and thermodynamics of cork. *J. Central South Univ. Forestry Technol*. 30(3):114–117.

Yao, F., Q. Wu, Y. Lei, W. Guo, and Y. Xu. 2008. Thermal decomposition kinetics of natural fibers: Activation energy with dynamic thermogravimetric analysis. *Polym. Degrad*. *Stabil*. 93(1):90–98.

Yao, F., Q. Wu, and D. Zhou. 2009. Thermal decomposition of natural fibers: Global kinetic modeling with nonisothermal thermogravimetric analysis. *J. Appl. Polym. Sci*. 114(2):834–843.

Zhao, J. 2012. Research in expansion impurities removing technology and mechanisms of *Quercus variabilis* cork. Northwest A&F University, Yangling, China.

Zhao, J., D. Feng, Y. Lei, W. Zhang, and Y. Zhang. 2013. Cell structure and chemical components of sclereids and lenticels from *Quercus variabilis* cork. *J. Northwest A&F Univ*. 41(7):119–124.